

Recrystallization textures in tantalum sheet and wire

C.L. Briant^{a,*}, E. MacDonald^a, R.W. Balliett^b, T. Luong^b

^a *Division of Engineering, Brown University, Providence, Rhode Island 02912, USA*

^b *H.C. Starck, Inc., 45 Industrial Place, Newton, MA, USA*

Received 8 March 1999; accepted 16 August 1999

Abstract

This paper presents a study of the evolution of recrystallization texture in tantalum. Both rolled sheet and drawn wire are considered. The rolled product developed a recrystallized texture in which the rolling plane normal was parallel to $\langle 111 \rangle$. There was no specific direction parallel to the rolling direction; rather this direction varied so that the rolling plane orientation could be accommodated. In the drawn wire, the recrystallized texture was one in which $\langle 110 \rangle$ was parallel to the deformation direction. © 2000 Elsevier Science Ltd. All rights reserved.

Keywords: Tantalum; Texture; Recrystallization; EBSP

1. Introduction

Although in many cases polycrystalline, body-centered-cubic (bcc) materials show reasonably isotropic mechanical properties, they can, through repeated deformation, become highly textured. The presence of this texture means that mechanical test samples cut out of the deformed piece will have varying mechanical properties that depend on the orientation of the test sample relative to that of the original piece. Production of wire and sheet products requires repeated deformation and is almost always accompanied by the development of a strong texture. Recrystallization of the worked material will not necessarily remove this texture, since research has shown that recrystallized samples may retain the texture of the worked material or develop a completely different texture through the formation and growth of new grains [1]. Furthermore, the amount of deformation that the sample receives may affect the sharpness and orientation of the texture that forms during recrystallization.

This paper reports a study of the recrystallization texture of tantalum. This material was processed from ingot to either a sheet or wire product. Samples were collected at various points during the process so that the evolution of the texture could be followed. The results show that a strong texture is formed in the recrystallized

sheet material in which the rolling plane is parallel to the $\{111\}$ plane in the material. There is not a preferred direction parallel to the rolling direction. The recrystallization texture increases in sharpness as the deformation continues. In the wire product the recrystallization texture is similar to the traditional bcc wire texture with $\langle 110 \rangle$ parallel to the drawing direction. However, this texture is not as strong as that in the sheet material.

2. Experimental

All of the samples used in this study were prepared by H.C. Starck. The material began as two cylindrical ingots that had been prepared by the process outlined in Fig. 1(a). The original powder and recycled material was first electron beam melted. These ingots were forged and then vacuum arc re-melted to produce the starting material. Their chemistries are given in Table 1. Before any processing was performed, samples were taken from the bottom and the top of each ingot in the manner depicted in Fig. 2.

Eight samples were collected that covered the diameter from one edge to another. As shown in the figure, they were taken so that the direction of growth of the columnar grains could be examined. In addition, each ingot was cut into two pieces and an additional set of eight samples was taken from one of these cut faces.

* Corresponding author. Fax: +1-401-863-1157.

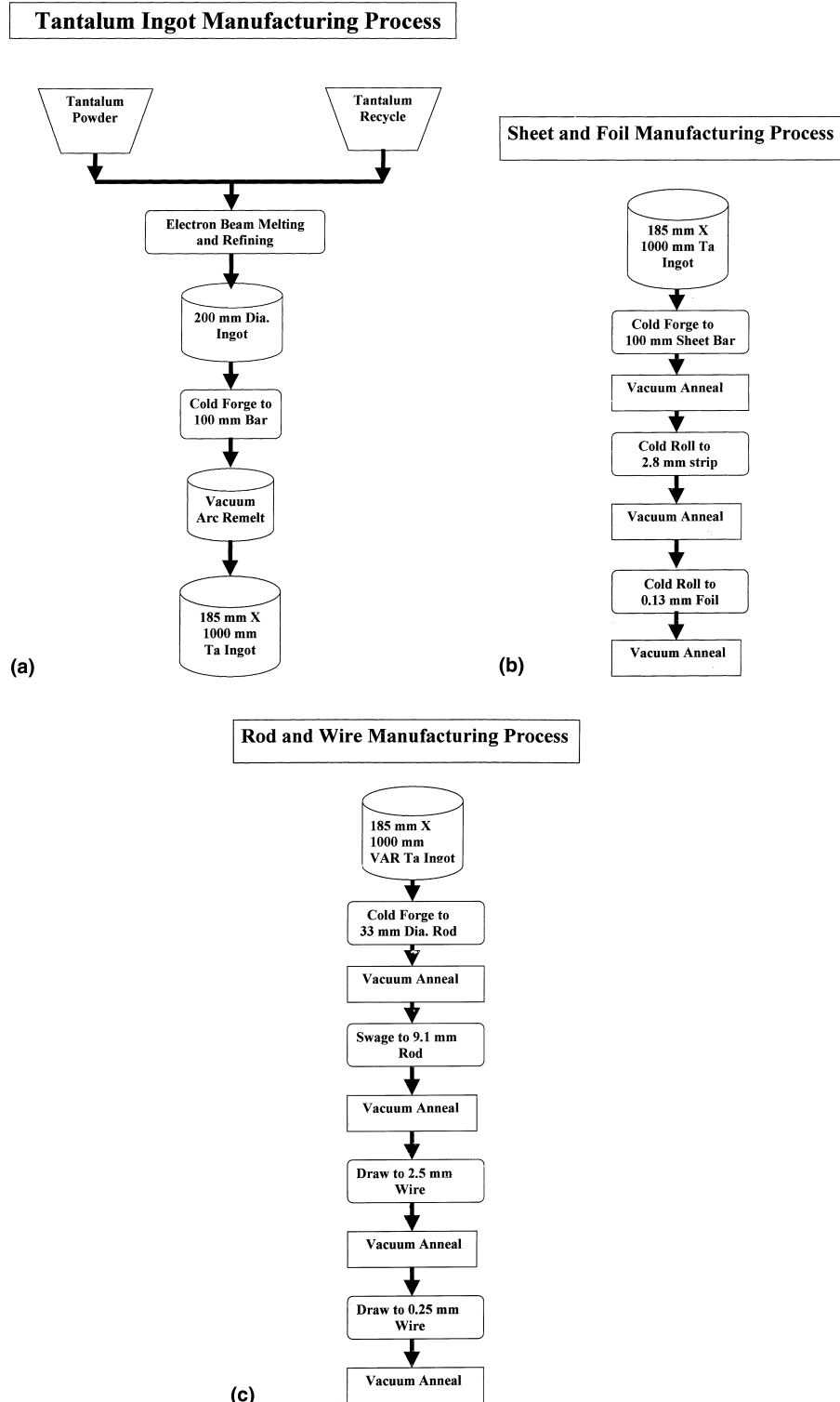


Fig. 1. (a) The manufacturing process for preparing tantalum ingots. (b) The manufacturing process for making foil from the ingot. (c) The manufacturing process for making rod and wire from the ingot.

Thus samples were prepared from the top, middle, and bottom of both of the original ingots. However, this paper reports results obtained only on samples taken from the middle of the ingots.

Ingot A was processed down to 0.13 mm thick sheet. The schedule is shown in Fig. 1(b). Samples were taken of the cold forged sheet bar as well as recrystallized samples of 2.8 and 0.13 mm thick sheet. Ingot B was

Table 1
Chemical composition of ingots (ppm)

Ingot	O	N	C	S	H	Fe	Ni	Cr	Cu	Ca	Si	Na	K	Y	Ta
A	2	10	<5	<5	<1	18	29	8	<1	<2	<8	<1	<10	<10	Bal.
B	10	18	<5	<5	<1	10	14	5	<1	<2	<8	<1	<10	<10	Bal.

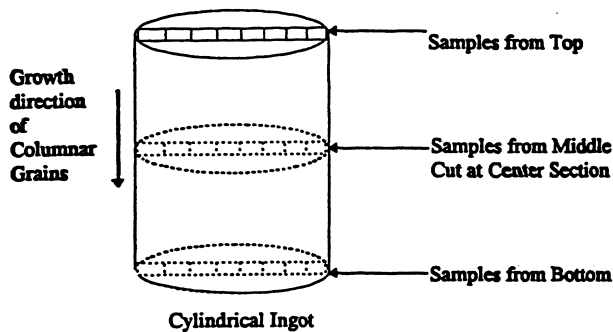


Fig. 2. The sampling procedure from the ingot. Samples were taken from the top and bottom, and then the ingot was cut in half and samples were taken from the middle. Note that enough samples were taken so that they spanned the entire diameter of the ingot.

processed to wire by the schedule shown in Fig. 1(c). Note that this schedule involved forging, swaging and wire drawing. Recrystallized samples were examined that had diameters of 9.1, 5, and 0.25 mm. The recrystallization treatments were vacuum anneals performed at a temperature of 1093°C for 1.5 h in a vacuum of 1×10^{-5} Torr.

The texture of the samples was determined by analyzing the Kikuchi patterns obtained from back-scattered electrons in the scanning electron microscope. This technique, which is often referred to as electron back-scattering diffraction pattern analysis (EBSP), allows one to determine texture by sampling the orientation of individual grains. The spatial resolution of this technique is approximately 1 μm , so by simply obtaining orientation information on many different grains one can determine the overall texture of the sample. The EBSP equipment was manufactured by Nordif, Inc. that was installed on a JEOL 845 scanning electron microscope. Details of this equipment and the technique have been given in a previous publication [2].

The data collected by this technique can be presented as a pole figure or an inverse pole figure. To construct the pole figure, one orients the basic circle of the stereographic projection with the geometry of the sample that is to be analyzed. The axes of the basic circle are identified with specific directions on the sample, such as the rolling direction or drawing direction. That is, a coordinate system is applied to the sample, and this same coordinate system defines the North–South and East–West directions on the pole figure. One then selects

a specific crystallographic direction, such as $\langle 110 \rangle$ and determines the orientation of that direction in different grains with respect to the general sample directions that one has chosen. This relative orientation is then plotted on the pole figure in the same way that one plots points on a stereographic projection. In all of the pole figures presented in this paper, the N–S axis will be the deformation direction. In the rolled samples the E–W axis will be the transverse direction and the normal to the figure will be parallel to the rolling plane normal.

The inverse pole figure is constructed differently. Here the plane of reference is always the surface of the sample that is being analyzed. One then plots in a standard triangle the specific crystallographic direction in the analyzed grains that is parallel to a chosen direction on the sample surface. For example, an inverse pole figure might show the crystallographic direction that is parallel to the rolling direction in each grain that has been analyzed.

3. Results

3.1. Microstructural studies

It is important to begin the presentation by considering the microstructures of the samples. The starting ingots were very coarse grained. Fig. 3 shows a macrograph of a cross-section of an ingot similar to the ones used in this study. Note that several of the grains are several centimeters across and that they form a long columnar structure as a result of the melting operation. In the forged samples the material had a similar structure.

Samples that had been rolled to 2.8 mm in thickness and recrystallized had an equiaxed grain structure, as shown in Fig. 4(a). The overall grain size was approximately 50 μm . The final rolled product, which had a thickness of 0.13 mm, had a similar equiaxed microstructure, as shown in Fig. 4(b).

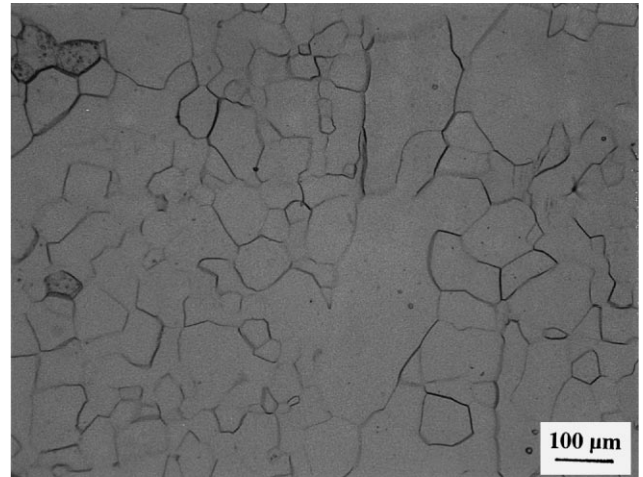
Samples that were swaged and drawn to a rod or wire product also had a recrystallized microstructure that consisted of equiaxed grains. Fig. 5(a) shows a micrograph of the sample drawn to a final diameter of 9.1 mm. The grains are very uniform across the transverse section and are approximately 20 μm in diameter. The

VAR Tantalum Ingot Section

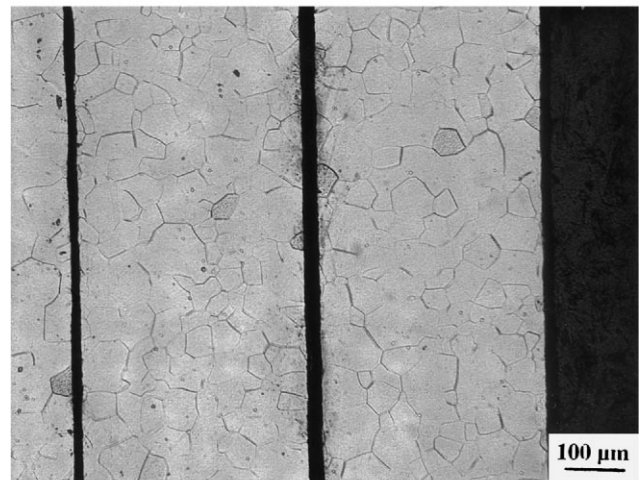


Fig. 3. A macrograph of a tantalum ingot.

material swaged to 5 mm had a similar structure, although the grain size was slightly smaller. Fig. 5(b) shows the microstructure of the sample drawn to a final diameter to 0.25 mm. It also contained equiaxed grains and a grain size of approximately 10 μm .



(a)

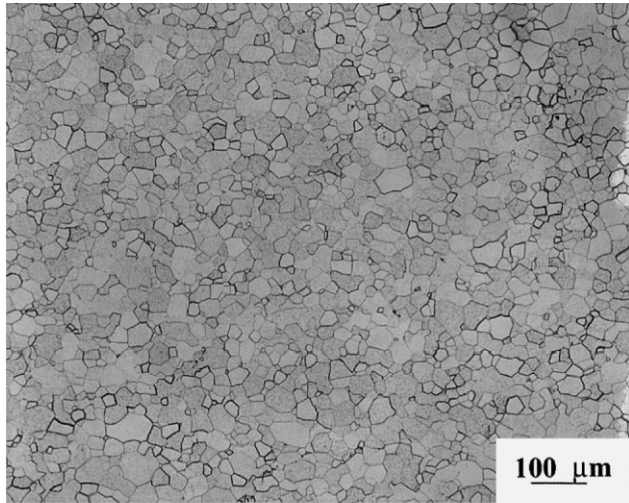


(b)

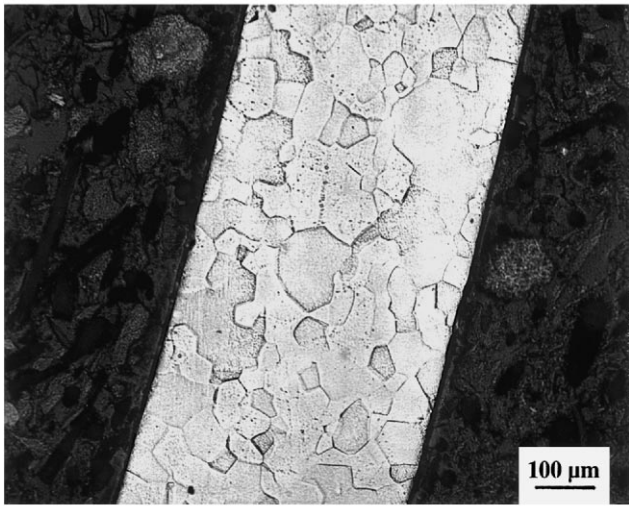
Fig. 4. Optical micrographs of recrystallized rolled sheet: (a) 2.8 mm thick sheet; (b) 0.13 mm thick sheet.

3.2. Texture analysis

As can be observed by examining Figs. 2 and 3, most of the individual samples from the ingot contained only two to four grains. A pole figure or inverse pole figure taken from an individual sample contained only a few clusters of points, with each cluster arising from the individual grains. Therefore, it is best to examine results from the entire series taken across the middle section of the ingot. These are shown in Fig. 6(a)–(h). This figure shows the inverse pole figures taken in a direction parallel to the growth direction of the grains; the figures, in order of Fig. 6(a)–(h), span the diameter of the ingot, with Fig. 6(a) and (h) representing the texture in the two outside samples. These results show that there is variation in the orientation of the different grains and that there is no single, obvious growth direction for the dendrites. However, we note that in the center of the



(a)



(b)

Fig. 5. Optical micrographs of samples of recrystallized cylindrical product: (a) 9.1 mm diameter rod; (b) 0.25 mm diameter wire.

sample there tends to be an alignment of the points along an axis between the $\langle 001 \rangle$ and $\langle 110 \rangle$ poles.

The next set of samples are those taken from the forged sheet bar. The collection scheme for each sample is shown in Fig. 7(a). The samples covered the entire cross-section of the forged ingot, but there are now two directions of interest. These are the growth direction of the dendrites in the ingot and the direction of the forging axis. Fig. 7(b) shows inverse pole figures taken along these two directions; the set of inverse pole figures in each figure are arranged in order from one side of the sheet bar to the other. In the inverse pole figures taken along the growth direction, one still notes that in the center of the sample there is a tendency for the directions to lie between the $\langle 001 \rangle$ and $\langle 110 \rangle$ poles as was found in the ingot. However, in the forging direction another texture component is observed. The grains tend

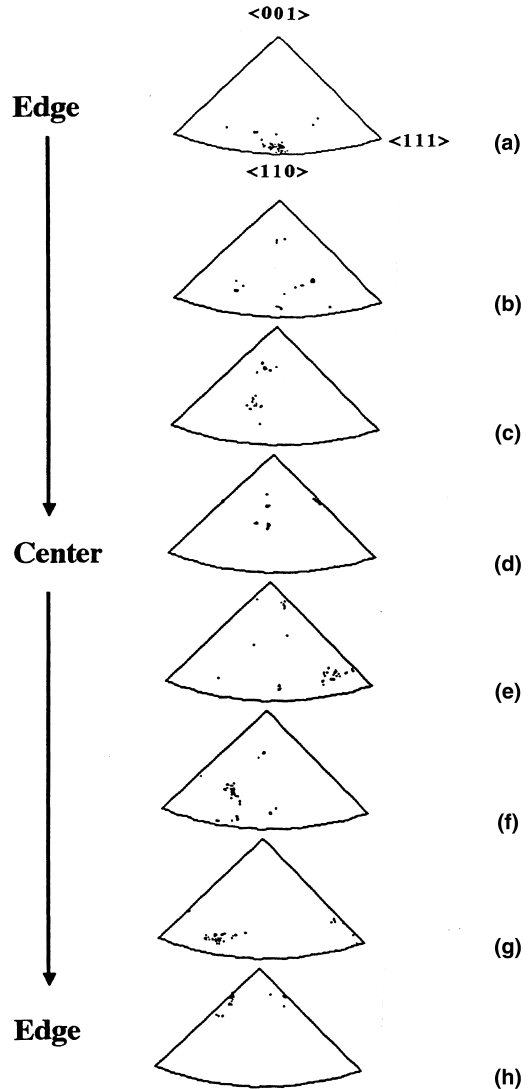


Fig. 6. Inverse pole figures of the ingot taken in the direction of growth of the columnar grains. These were taken from the middle of the ingot. Note that the progression from Fig. 6(a)–(h) represents inverse pole figures from samples taken in order from one side of the ingot to the other. Fig. 6(a) shows the directions on the stereographic triangle.

to be oriented so that the forging direction is located between the $\langle 001 \rangle$ and $\langle 111 \rangle$ pole.

After the sample was rolled to 2.8 mm thick sheet and recrystallized, a strong texture was observed. Fig. 8(a) shows the $\langle 110 \rangle$ pole figure for this sample and Fig. 8(b) and (c) show inverse pole figures taken in directions parallel to the rolling plane normal and the rolling direction, respectively. The texture in the rolling direction is somewhat centered around $\langle 110 \rangle$ but clearly there is a significant amount of scatter. The direction parallel to the rolling plane normal is aligned between $\langle 001 \rangle$ and $\langle 111 \rangle$. This alignment is shown in a unit cube in Fig. 8(d). When the sample is further rolled to 0.13 mm thick sheet, the recrystallization texture is even stronger.

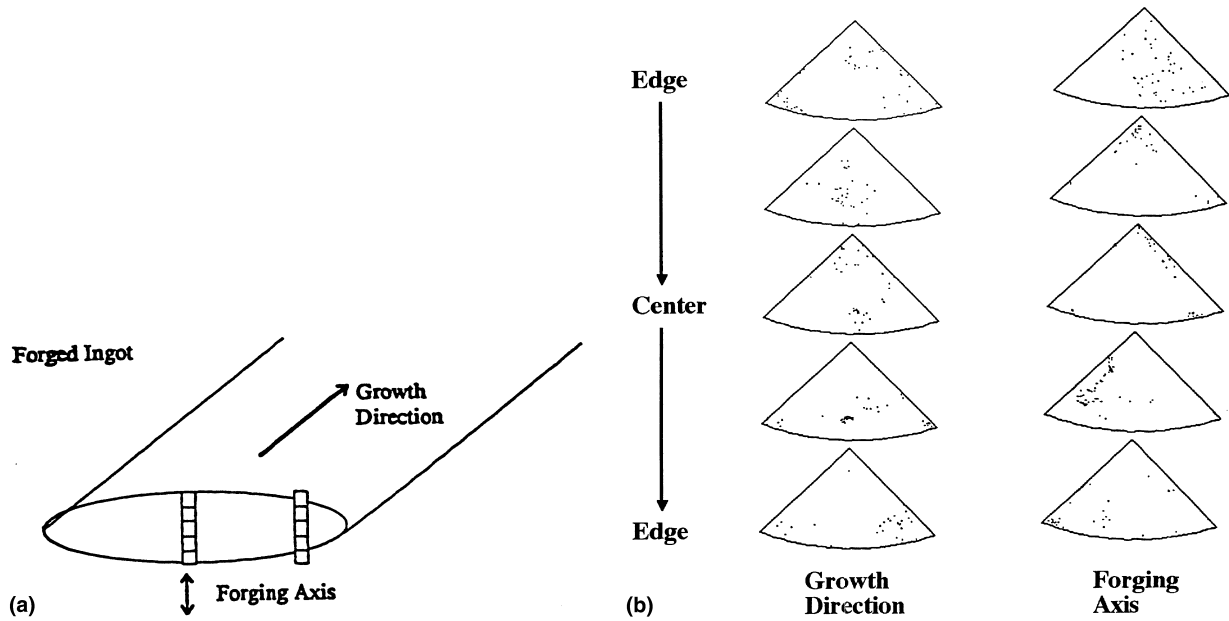


Fig. 7. (a) The sampling procedure for the forged sheet bar. (b) The inverse pole figures taken in the direction parallel to the growth axis of the columnar grains and in the direction parallel to the forging axis. Note that the progression from the top inverse pole figure in each column to the bottom represents a progression across the forged sheet bar from the top to the bottom, as indicated by the sampling procedure shown in Fig. 7(a). The orientations on the stereographic triangle are the same as those shown in Fig. 6.

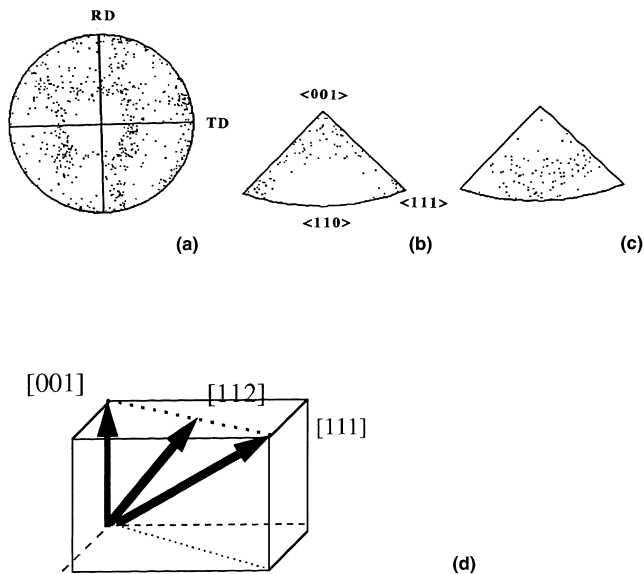


Fig. 8. Texture information for the rolled and recrystallized 2.8 mm thick sheet. (a) The $\langle 110 \rangle$ pole figure. The rolling direction is parallel to the N–S axis of the pole figure and the transverse direction is parallel to the E–W axis of the pole figure. (b) The inverse pole figure taken in a direction parallel to the rolling plane normal. (c) The inverse pole figure taken in a direction parallel to the rolling direction. (d) A unit cube showing the $[001]$, $[112]$, and $[111]$ directions.

Fig. 9(a) shows the $\langle 110 \rangle$ pole figure and Fig. 9(b) and (c) show the inverse pole figures for directions parallel to the rolling plane normal and the rolling direction, respectively. It is clear that the rolling plane normal is now

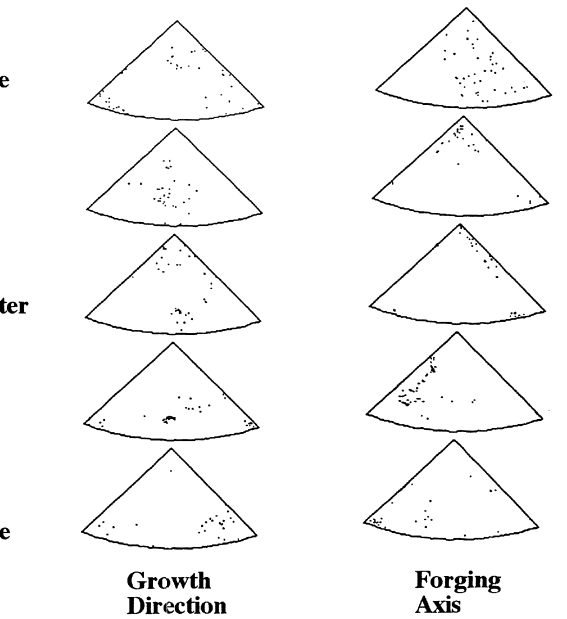


Fig. 9. Texture information for the rolled and recrystallized 0.13 mm thick sheet. (a) The $\langle 110 \rangle$ pole figure. The rolling direction is parallel to the N–S axis of the pole figure and the transverse direction is parallel to the E–W axis of the pole figure. (b) The inverse pole figure taken in a direction parallel to the rolling plane normal. The directions on this inverse pole figure are the same as those shown in Fig. 8(b). (c) The inverse pole figure taken in a direction parallel to the rolling direction. The directions in this inverse pole figure are the same as those shown in Fig. 8(b).

parallel to the $\langle 111 \rangle$ direction and that there is no particular direction parallel to the rolling direction, a result consistent with the presence of a $\langle 111 \rangle$ γ -fiber. The texture in the rolling direction is sacrificed to allow the rolling plane normal to achieve this orientation.

The other set of samples were those swaged and drawn to a round product prior to recrystallization. Fig. 10(a)–(c) shows inverse pole figures of recrystallized samples of material that had diameters of 9.1, 5, and 0.25 mm, respectively. These inverse pole figures were taken in a direction parallel to the deformation direction, since that is the only well-defined direction in a cylindrical sample. All three pole figures show a $\langle 110 \rangle$ texture, with this texture being the strongest in the

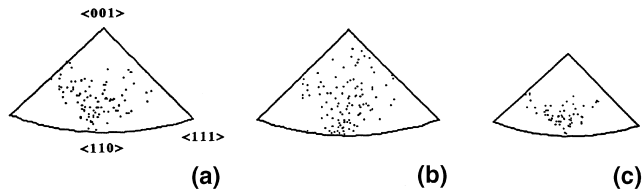


Fig. 10. Inverse pole figures for recrystallized cylindrical product. All inverse pole figures were taken parallel to the deformation direction: (a) 9.1 mm diameter wire; (b) 5 mm diameter wire; (c) 0.25 mm diameter wire.

sample deformed to the smallest diameter. A comparison of these results with those shown in Fig. 9 suggest that the recrystallization texture is not as strong in the cylindrical product as in the sheet product.

4. Discussion

The results presented above show the evolution of the texture in the recrystallized sheet and wire. Some of these observations are now considered in more detail.

The first issue that we would like to describe is the growth direction of the large columnar grains in the ingot. The inverse pole figures suggested that the growth direction of these grains varied between $\langle 001 \rangle$ and $\langle 110 \rangle$, although there is significant scatter around these directions. However, research has shown that in bcc materials the growth direction of dendrites is usually $\langle 001 \rangle$, so these results would be reasonably consistent with that information [3]. Furthermore, the macrograph of the ingot indicates that the grains are curved, but the mounts were taken perpendicular to the external dimensions of the ingot. Thus the actual growth direction may have been at an angle to the mount.

The results in Fig. 7 showed that forging imparted a texture in the direction parallel to the forging axis. This texture is most pronounced in the region of the sample that was originally composed of the long columnar grains. In the original center of the ingot, a texture has formed, but this textured material is surrounded on the outside by grains in which the texture is not as strong. The particular texture that forms is one in which the direction parallel to the compression axis varies along the side of the standard triangle from $\langle 001 \rangle$ to $\langle 112 \rangle$ to $\langle 111 \rangle$. All three of these deformation textures have been observed in tantalum and the study of texture evolution during compression by Wright et al. [4] indicated that during compression the $\langle 001 \rangle$ and $\langle 111 \rangle$ directions tend to align parallel to the compression axis, in agreement with our findings.

The rolled and recrystallized sheet samples showed that the recrystallization texture was such that the rolling plane normal was parallel to $\langle 111 \rangle$ but that this orientation was achieved at the expense of any texture in

Table 2
Texture information on rolled and recrystallized tantalum

Reference	Sheet thickness (mm)	Annealing texture
[5]	0.0127	$\{111\}\langle 112 \rangle$
[4]	6.2	Edge $\{100\}\langle 001 \rangle$ Center $\{111\}\langle 110 \rangle$
[6]		$\langle 111 \rangle$ parallel to rolling plane
[7]	4.6	$\{111\}\langle 112 \rangle$ and $\{111\}\langle 110 \rangle$
[7]	4.6	$\{111\}\langle uvw \rangle$ and $\{100\}\langle uvw \rangle$
[8]	7.6	$\{111\}\langle uvw \rangle$ and $\{100\}\langle 011 \rangle$
[9]		$\{111\}\langle 110 \rangle$

the rolling direction. Both the inverse pole figures and the $\langle 110 \rangle$ pole figures demonstrate this orientation. The circle of points that is observed on the pole figure arise from the fact that the $\langle 111 \rangle$ direction must remain normal to the pole figure but that the $\langle 110 \rangle$ poles can be rotated 360° around this direction if no other requirement is made on their orientation. The grain growth process that occurs during recrystallization is such that this texture is favored. Furthermore, the data in Table 2 indicated that similar results have been found by other researchers.

In the swaged and drawn samples, the recrystallization texture was such that the $\langle 110 \rangle$ direction was parallel to the deformation direction. This texture has been found in other drawn and recrystallized bcc metals [1].

5. Conclusions

The conclusions of this study are the following:

1. The ingots examined in this study had large columnar central grains. The growth direction for these grains varied, with some scatter between $\langle 001 \rangle$ and $\langle 110 \rangle$ in the standard triangle.
2. Forging the ingots into an elliptical shape caused the development of a texture in the direction parallel to the compression axis.
3. Rolling the samples to a final sheet of thickness 0.13 mm followed by recrystallization caused the formation of a recrystallization texture with the rolling plane normal parallel to $\langle 111 \rangle$.
4. Swaged and drawn samples that were recrystallized had a $\langle 110 \rangle$ texture.

Acknowledgements

The texture analysis work performed at Brown University was supported by H.C. Starck. The instruments used for this analysis are maintained by the NSF supported Materials Research Science and Engineering Center at Brown University.

References

- [1] Barrett CS, Massalski TB. *Structure of Metals*. New York: McGraw-Hill, 1966.
- [2] Bai R, Briant CL, Paine DC, Beresford JR. *Metall Mater Trans A* 1998;29:757.
- [3] Chalmers B. *Trans AIME* 1954;200:519.
- [4] Wright SI, Gray III GT, Rollett AD, *Metall Mater Trans A* 1994;25A:1025.
- [5] Pugh JW, Hibbard Jr. WR. *Trans ASM* 1956;48:529.
- [6] Schwartz AJ, Lassila DH, LeBlanc MM. *Mater Sci Eng* 1998;A244:178.
- [7] Clark JB, Garrett Jr. RK, Jungling TL, Asfahani RI. *Metall Trans A* 1991;22:2959.
- [8] Clark JB, Garrett Jr. RK, Jungling TL, Vandermeer RA, Vold CL. *Metall. Trans. A* 1991;22:2039.
- [9] Raabe D, Schlenker G, Weisshaupt H, Lucke K. *Mater Sci Technol* 1994;10:299.